Inorganic Chemistry

ARTICLE

pubs.acs.org/IC

First Experimental Evidence of a New D4-$AgCoO_2$ Delafossite Stacking

R. Berthelot,[†,‡] M. Pollet,[*,†] J.-P. Doumerc,[†] and C. Delmas[†,§]

[†]CNRS, Université de Bordeaux, ICMCB, 87 avenue du Dr. A. Schweitzer, 33608 F - Pessac, France

[‡]CEA-Grenoble, DRT-LITEN, 17 rue des Martyrs, 38054 Grenoble, France

[§]CNRS, ENSCBP, ICMCB, 87 avenue du Dr. A. Schweitzer, 33608 F - Pessac, France

ABSTRACT: A new polytype of $AgCoO_2$ delafossite has been prepared from the ordered OP4-(Li/Na)CoO_2 layered compound using ion-exchange reaction in molten salts. As expected from the structural model assuming a topotactic process, the lamellar structure of this new polytype is an alternate combination of the already known 2H and 3R delafossite polytypes. It crystallizes in the $P6_3/mmc$ space group with cell parameters $a_{hex.}$ = 2.871(1) Å and $c_{hex.}$ = 24.448(1) Å. Thermal stability, morphology characterization, and electrical properties are reported here and compared with those of the 2H and 3R $AgCoO_2$ polytypes.

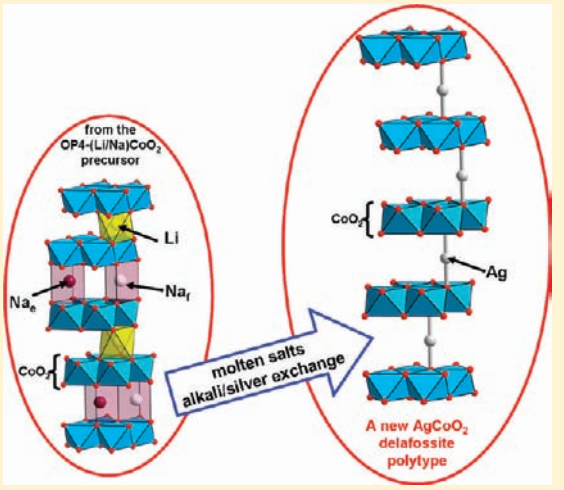

1. INTRODUCTION

Delafossite compounds refer to the ternary oxides AMO_2 with a structure described as a stacking of MO_6 edge-shared octahedra slabs linked together by linearly coordinated A atoms. The archetype named after G. Delafosse is the mineral $CuFeO_2$ with layers of $Cu^{I}O_2$ dumbbells between $Fe^{III}O_6$ octahedra sharing edges and forming FeO_2 slabs.[1,2] Typical A cations are monovalent Cu, Ag, Pd, and Pt, and possibly divalent Hg.[3−7] The M element is generally a trivalent metal or a rare earth when A = Hg.[8] Most delafossite oxides are insulators or semiconductors for A = Cu and Ag (apart from $AgNiO_2$) or metallic for A = Pt and Pd[4,9,10] and for Ag_nNiO_2 (n = 1, 2).[11−17] The difference between the several polytypes lies in the oxygen stacking along the c-axis of the hexagonal cell. Most of the reports are mainly dealing with the so-called 2H and 3R polytypes depending whether the oxygen atoms' packing is AB-BA or AB-BC-CA where the letters A to C refer to the usual three available triangular positions in an oxygen close packing (Figure 1). Their respective space groups are $P6_3/mmc$ and $R\bar{3}m$. Another 6H stacking was also reported.[18−22] To standardize the description of these lamellar AMO_2 oxides, the nomenclature proposed by Delmas et al. to distinguish the different alkali layered polytypes[23] will be followed hereafter. It consists on a letter that stands for the intercalation site symmetry of the A element and on a figure corresponding to the number of MO_2 slabs in the hexagonal cell. A prime superscript can be used and refers to a monoclinic distortion of the unit cell. Using the D letter standing for the A cation in the Dumbbell coordination, the various delafossite polytypes will hereafter be referred as D2 for 2H and D3 for 3R *(D6 for 6H)*.

The main difference between the D2 and the D3 structures consists in the orientation of the successive MO_2 slabs. In the D2 type all the M cations are superimposed along the c-axis and each MO_2 slab is rotated by $\pi/3$ versus the previous one (Figure 1a). Therefore, the structure is described with two basic blocks: M_c-O_B-A_b-O_B-(M_c) and M_c-O_A-A_a-O_A-(M_c). On the contrary in the D3 packing, all the MO_2 slabs have the same orientation (Figure 1b), and the structure is described with three blocks: M_c-O_B-A_b-O_B-(M_a), M_a-O_C-A_b-O_C-(M_b), and M_b-O_A-A_b-O_A-(M_c).

Because of this difference of packing, a transition from the D2 structure to the D3 one is not possible by a topotactic process and requires breaking Co−O bonds.

High-temperature synthesis of silver delafossites using classic ceramic methods never occurs in open systems because Ag_2O decomposes owing to its low free energy of formation.[3,24] Von Stählin and Ostwald were the first to report the synthesis of the D3-$AgCoO_2$ polytype using a hydrothermal process.[20] In a series of significant papers about the delafossite compounds family, Shannon, Rogers, and Prewitt confirmed this work with the synthesis of black hexagonal plate-like single crystals of $AgCoO_2$.[3−5] However, they also proposed an alternative method based on ionic exchange in molten salts using lamellar O3-$LiCoO_2$ as precursor

Received: February 3, 2011
Published: April 18, 2011

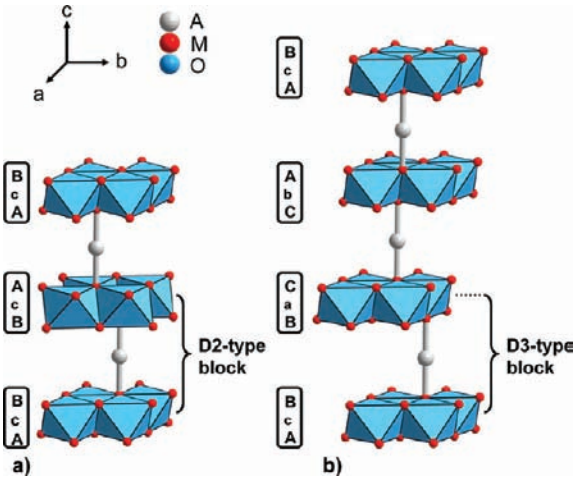

Figure 1. Perspective representation of the D2 (2H) (a) and D3 (3R) (b) delafossite AMO_2 stacking. The difference between the two polytypes arises from the oxygen atoms stacking sequence (capital letters) and from the orientation from one MO_2 slab to another. Cobalt atoms' positions are indicated in lower-case letters. For convenience only one A ion is shown in each interslab space.

material. The resulting silver delafossite is also the rhombohedral D3 polytype. The hexagonal polytype synthesis was later reported by Shin et al. using P2-$Na_{\sim 0.7}CoO_2$ as precursor in a similar ionic exchange.[12−14] Recently Muguerra et al. proposed a similar result with a slight change in the salt composition.[25]

These previous results clearly show that the ionic exchange process occurs through a topotactic mechanism: the oxygen sequence of the initial alkali layered precursor directly impacts on the obtained $AgCoO_2$ polytype.

On the basis of this observation, we have studied such an ionic exchange starting from the ordered OP4-$Li_xNa_yCoO_2$ layered compound that we have recently reinvestigated.[26] This material exhibits an alternate combination of P2-type sodium and O3-type lithium blocks along the hexagonal *c*-axis[27−30] (Figure 2a) from which we could predict a new packing combining both D2 and D3-type blocks (Figure 2c). We are reporting on the description of this new D4-$AgCoO_2$ delafossite polytype, its thermal stability, and the comparison of some electronic properties with those of the already known D2 and D3 polytypes. For consistency, D2 and D3 samples were prepared using similar protocols.

2. EXPERIMENTAL SECTION

2.1. Synthesis of the Precursors. P2-$Na_{\sim 0.7}CoO_2$ and O3-$LiCoO_2$ were obtained from solid-state reactions using dry alkali carbonates and cobalt oxide Co_3O_4 precursors that were intimately ground together. Stoichiometric ratio was used for the preparation of O3-$LiCoO_2$ while an excess of 5 wt % of sodium carbonate was added for the preparation of P2-$Na_{\sim 0.7}CoO_2$ to balance to sodium loss at high temperature. These mixtures were respectively heated at 850 and 900 °C for 24 h under oxygen flow with heating and cooling rates set to +2 °C min^{-1} and −5 °C min^{-1}, respectively.

The P′3-$Na_{\sim 0.6}CoO_2$ compound was obtained by mixing cobalt oxide Co_3O_4 and sodium peroxide Na_2O_2 (15 wt % excess to avoid Co_3O_4 traces) in an argon-filled glovebox.[31−33] The mixture was then heated at 550 °C for 12 h under oxygen flow.

In each case, typical batches of 7 g were produced.

Several authors have reported on the synthesis of OP4-$Li_xNa_yCoO_2$ compounds with some nuances in the synthesis protocol, and most of them agree on the difficulty to obtain the pure compound.[27−30] In a recent paper we thoroughly reinvestigated the synthesis path and proposed a more efficient protocol. In brief, O3-$LiCoO_2$ and P2-$Na_{\sim 0.7}CoO_2$ precursors, prepared as described above, were intimately mixed together in an argon-filled glovebox in the molar proportions 42/58 to obtain a pure $Li_{0.42}Na_{0.41}CoO_2$ phase (the alkali stoichiometric phase was previously shown to not be reachable this way[26]). The mixture was put into a gold tube which is sealed and heated at least 1 day at ∼920 °C in a preheated furnace. The tube was finally quenched in a water bath. The reaction is total, and roughly 3 g are produced at once.

As all these compounds are moisture sensitive, they were stored in dry atmosphere before performing the ion-exchange reactions.

2.2. Ion-Exchange Process. Focusing on exchange methods, the D3-$AgCoO_2$ polytype is obtained in the literature from the O3-$LiCoO_2$ precursor, but it is difficult to reach a complete ion-exchange as some residual precursor often remains in the final product. This is related to a more complex mechanism for the exchange that requires (i) a big change in the interslab thickness and (ii) a slab gliding. Moreover the ion diffusion through octahedra is more difficult than through a trigonal prism. To bypass this problem and maximize the purity of the D3 compound, the P′3-$Na_{\sim 0.6}CoO_2$ precursor was used. Following previous works dealing with silver delafossite synthesis,[12−14,34−36] ionic exchanges in molten salts were performed by mixing 300 mg of the precursors (i.e., OP4-(Li/Na)CoO_2, P2-$Na_{\sim 0.7}CoO_2$ or P′3-$Na_{\sim 0.6}CoO_2$) with silver nitrate and potassium nitrate. A preliminary ball-milling step was performed on the OP4-(Li/Na)CoO_2 powder to reduce the average grain size and to facilitate the $(Li^+ + Na^+)/Ag^+$ exchange (milling characteristics: ten times 10 min at 500 rd min^{-1}). For the three cases, a large excess of silver nitrate (5 times more than the alkali nominal content) was used to promote the ion-exchange process. The addition of potassium nitrate in the molar ratio $AgNO_3/KNO_3 = 3/2$ lowers the salt melting point down to ∼130 °C[37] and increases its volume which promotes the ionic exchange. The mixtures were heated at 300 °C under air during 15 h; the final products were then washed in water to remove the remaining nitrates and finally oven-dried overnight.

2.3. Characterizations. X-rays diffraction (XRD) measurements were performed using a PANalytical X'Pert Pro powder diffractometer in the Bragg−Brentano geometry using copper Kα radiation. Data were collected using an X'Celerator detector in a 5−100° window.

The cation ratios and also the chemical composition in the case of the alkali based precursors were determined by Inductively Coupled Plasma Absorption Electron Spectroscopy (ICP-AES) on a Varian 720-ES. Powder samples (∼10 mg) were dissolved in an acid solution heated to ∼70 °C (HCl was used for alkali layered precursors, HNO_3 was used for silver-based compounds to avoid AgCl formation).

Scanning electron microscopy (SEM) analysis was performed on the delafossite compounds with a Hitachi S-4500 field emission microscope. To avoid charging, the powder samples were preliminary metalized by Pd cathodic sputtering (1 min, 10 mA).

Thermogravimetric analysis (TGA) was performed with an STD Q600 apparatus under an Ar flow (initial dwell of 2 h. at 100 °C, heating rate 5 °C min^{-1}, final dwell of 30 min at 600 or 800 °C, cooling rate 5 °C min^{-1}).

To quantify the ball-milling efficiency, the average grain size of the OP4-(Li/Na)CoO_2 powder samples was determined before and after the milling with a Malvern Mastersizer 2000 particle size analyzer by immersing the powder in an ethanol bath, with a preliminary ultrasonic step to break up the biggest aggregates. The $D_V(0.5)$ values that will be given in this paper refer to the volume median diameter.

Transport properties of the delafossite compounds were measured only on non-sintered compacted pellets (compactness close to 70%). Electrical direct current (DC) resistivity measurements were performed with the four-probe method in the 4−300 K range, and the thermoelectric power was measured with a homemade equipment.[38]

dx.doi.org/10.1021/ic2002354 |*Inorg. Chem.* 2011, 50, 4529–4536

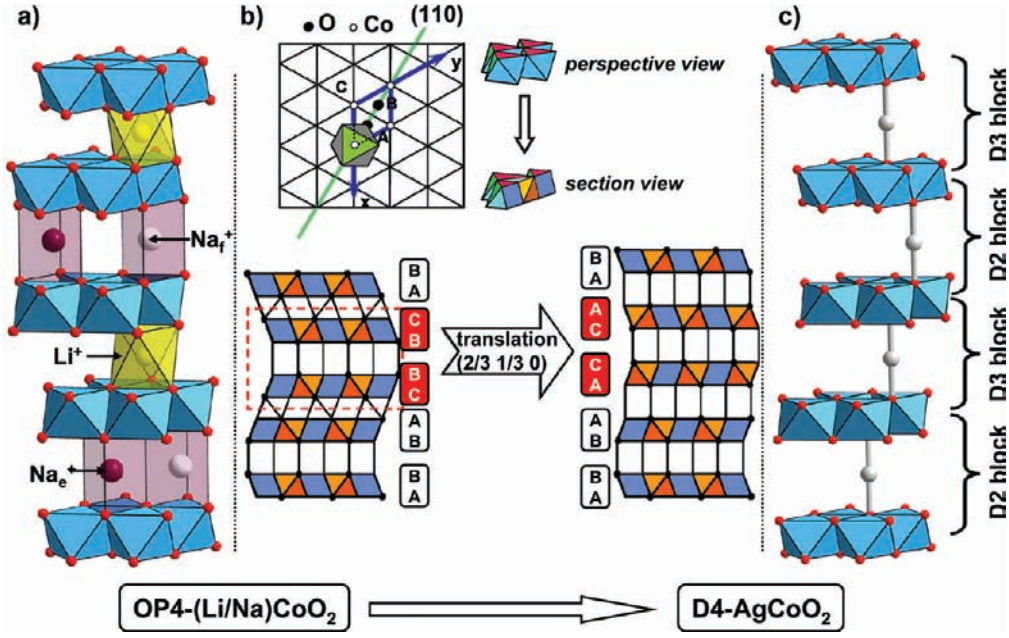

Figure 2. Perspective representation of the OP4-(Li/Na)CoO_2 precursor (a) and of the delafossite D4-$AgCoO_2$ (c) that can be obtained by ionic exchange. For the OP4 stacking, lithium ions occupy octahedral sites (in yellow), while sodium ions are intercalated in trigonal prisms sharing either faces (in white) or edges (in purple) with surrounding CoO_6 octahedra. In (b), the projection with the [110] viewing direction evidence the block gliding which occurs during the OP4 → D4 transformation.

2.4. Simulation of the New D4 Stacking. A method similar to the one recently used to build up the O4-$LiCoO_2$ polytype[39] was used to sketch the D4 delafossite structure and to anticipate the stacking sequence and its basic crystallographic parameters. From the work of Seshadri et al. on the D3 polytype,[7] we obtained the thicknesses of both the CoO_2 slabs and AgO_2 interslab spaces, and we assumed that similar crystallographic data characterize the D2 polytype. We used this information as input parameters to build up the new blocks of the D4 polytype, which implicitly fixes the z position for both the cobalt and the oxygen ions. Starting from the OP4-(Li/Na)CoO_2 compound (Figure 2a), the $NaCoO_2$ block requires no symmetry adaptation since the D_{3h} environment of the sodium is compatible with the $D_{\infty h}$ environment of the silver. However, a (2/3 1/3 0) gliding of one CoO_2 slab over two is imposed in the $LiCoO_2$ sub-block to superimpose the oxygen atoms in the interlayer and create a $D_{\infty h}$ site (Figure 2b). This gliding is similar to the one required during the O3 → D3 ionic exchange. All the alkali ions are then replaced by silver ions that are directly located at the center of the dumbbell formed by 2 superimposed oxygen atoms. The $a_{hex.}$ cell parameter of the new structure is fixed to the one of D2 and D3 compounds (2.875 Å), while the $c_{hex.}$ parameter (24.499 Å) is 4 times the thickness of a single $AgCoO_2$ block. The crystallographic symmetry operator determination led to the $P6_3/mmc$ space group, and the corresponding simulated XRD pattern is presented in Figure 3a. The D2, D3, and D4 polytypes obviously offer many similarities such as slab and interslab space thicknesses, and the simulated XRD pattern of the D4 polytype is very close to the ones of the D2 and D3 compounds, especially in the low angle range (Figure 3). However, focusing on the 2θ positions of the diffraction peaks (105), (1011), and (1013) which are strong characteristic peaks of the D4 polytype, this latter can be clearly distinguished from the two other polytypes.

3. RESULTS AND DISCUSSION

3.1. Ion-Exchange Processes. Experimental XRD patterns (not presented here) confirm the synthesis of pure precursors OP4-(Li/Na)CoO_2, P2-$Na_{\sim 0.7}CoO_2$, P′3-$Na_{\sim 0.6}CoO_2$ with cell parameters in good agreement with the literature.[26,27,31,32]

As shown in Figure 3b, a pure D2-$AgCoO_2$ is obtained from the P2-$Na_{\sim 0.7}CoO_2$ phase. This result is confirmed with the ICP-AES titration that reveals a negligible Na/Co ratio and a ratio Ag/Co = 1.04(5), that is, it highlights the absence of remaining sodium precursor and evidence the complete Na^+/Ag^+ exchange. All the diffraction peaks can be indexed in the $P6_3/mmc$ space group, and the cell parameters are $a_{hex.}$ = 2.873(1) Å and $c_{hex.}$ = 12.229(4) Å, in total agreement with previous works.[14,25]

As shown in Figure 3c, a pure D3-$AgCoO_2$ is obtained from the P′3-$Na_{\sim 0.6}CoO_2$ phase. The space group is $R\bar{3}m$, and the cell parameters ($a_{hex.}$ = 2.872(1) Å and $c_{hex.}$ = 18.337(5) Å) are in good agreement with previous works.[3,7] Note that it is the first report on a D3-$AgCoO_2$ synthesis from the P′3 precursor. The very small monoclinic distortion, which characterizes the P′3 stacking,[33] does not affect the exchange mechanism.

To improve the $(Li^+ + Na^+)/Ag^+$ ionic exchange and to promote the D4-$AgCoO_2$ compound formation, the OP4-(Li/Na)CoO_2 precursor powder was first ground to reduce the grain size from $Dv_{(0.5)}$ ~40 μm to ~10 μm. After washing, the ICP-AES analysis leads to a ratio Ag/Co = 0.96(5) and to negligible alkali to Co ratios (0.01(5) and 0.02(5) for Li/Co and Na/Co respectively). The experimental XRD pattern shown in Figure 4 perfectly matches with the theoretical one presented in Figure 3a. In particular, the characteristic diffraction peaks (105), (1011), and (1013) of the D4 compounds are perfectly visible. According to the XRD pattern of the OP4-(Li/Na)CoO_2 compound,[26] there is no remaining trace of the layered precursor. A profile matching refinement shows that this compound crystallizes as expected in the $P6_3/mmc$ space group with $a_{hex.}$ = 2.871(1) Å and $c_{hex.}$ = 24.448(1) Å, in very good agreement with the theoretical data as summarized in Table 1. The significant line broadening results certainly from defects or constraints that may appear during

dx.doi.org/10.1021/ic2002354 |Inorg. Chem. 2011, 50, 4529–4536

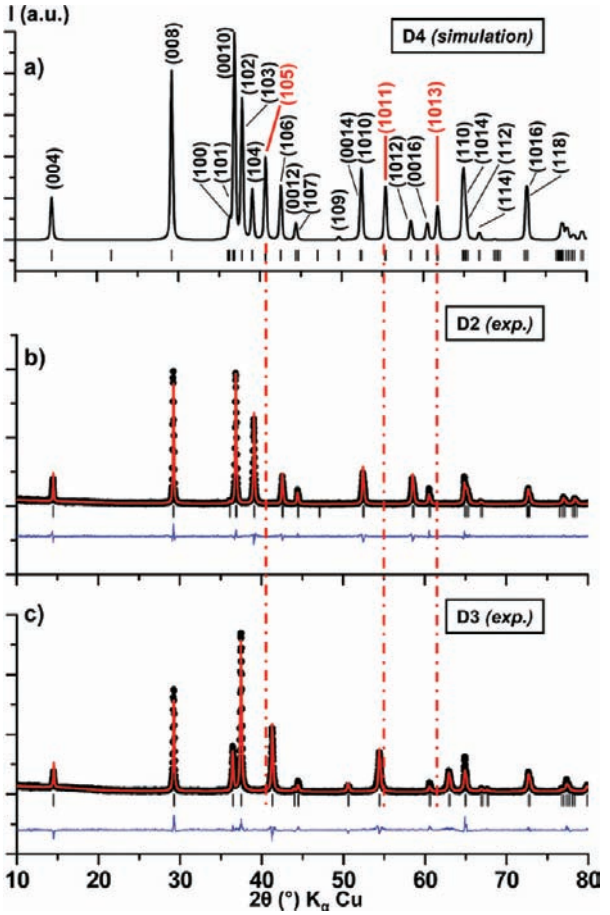

Figure 3. Comparison between (a) the simulated XRD pattern of the D4-$AgCoO_2$ delafossite polytype and the experimental powder patterns of (b) D2-$AgCoO_2$ and (c) D3-$AgCoO_2$; the observed (black points), refined by profile matching (red solid line) and difference (blue line) profiles as well as the Bragg position (vertical bars) are shown. The red dashed lines evidence the (105), (1011), and (1013) diffraction lines that are characteristic of the D4-$AgCoO_2$ phase and enable to distinguish this polytype from the other ones.

the structural reorganization preventing any Rietveld refinement. The atomic positions resulting from the simulation of the D4 stacking are anyway given in Table 1.

3.2. Scanning Electron Microscopy and Particle Size Analysis. Figure 5 compares the grain size morphology of the three obtained delafossite polytypes with SEM micrographs. The D2 material exhibits plate-like particles, for which the diameter ranges from 2 to 10 μm and with ~2 μm in thickness (Figure 5 a-b). Both the general hexagonal shape and the layered structure that characterize the P2-$Na_{\sim 0.7}CoO_2$ precursor[40] are clearly observed in the material after ionic exchange, with, in addition, well-defined edges in most of the cases. The grain size of the D3 sample is much lower (<1 μm), which may be explained by the lower synthesis temperature of P′3-$Na_{\sim 0.6}CoO_2$ precursor (550 as compared to 850 °C for the P2 one) (Figure 5 c-d). The grain morphology is here also characterized by quite well-defined edges. Because of the prior ball-milling sequence of the OP4 powder, the grain size of the resulting D4 delafossite is lower than for the other polytypes, with sizes down to few tenths of a nanometer for most of the particles (Figure 5 e-f). The layered character can only sporadically be observed on the biggest particles.

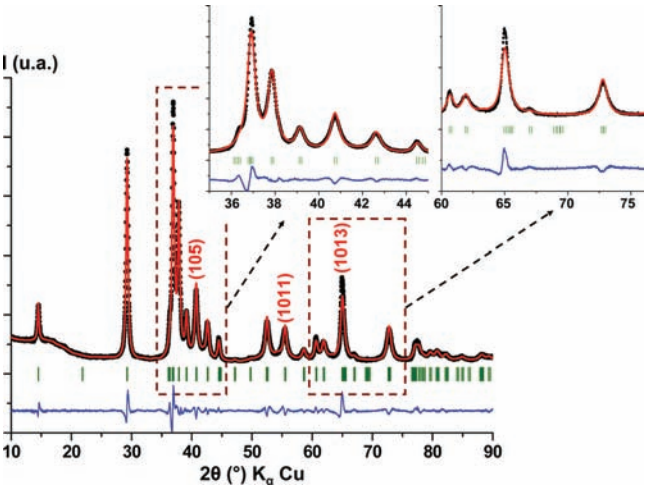

Figure 4. Profile matching refinement of the experimental powder XRD pattern of D4-$AgCoO_2$ obtained by ion-exchange from an OP4-(Li/Na)CoO_2 ball-milled powder. The observed (black points), calculated (red solid line) and difference (blue line) profiles as well as the Bragg positions (green bars) are shown. Refined cell parameters are given in Table 1.

Table 1. Atomic Positions of the D4-$AgCoO_2$ Structure Resulting from the D4 Stacking Simulation and Refined Cell Parameters Obtained from the XRD Pattern Shown in Figure 4′[a]

parameters used for the simulation					
$P6_3/mmc$		$a_{hex.}$ = 2.875 Å		$c_{hex.}$ = 24.499 Å	
atomic positions					
atom	site	*x*	*y*	*z*	occ.
Ag1	2a	0	0	1/2	1
Ag2	2d	1/3	1/3	3/4	1
Co	4f	2/3	1/3	5/8	1
O1	4e	0	0	0.5858	1
O2	4f	1/3	2/3	0.6642	1
Experimental Profile Matching Refinement					
$a_{hex.}$ = 2.871(1) Å				$c_{hex.}$ = 24.448(1) Å	

[a] The small difference between the simulated and experimental lattice parameters confirms the reliability of the simulation.

Note finally that while the particle distribution appears quite narrow for the D2 polytype, it is very broad in the case of the D3 and D4 polytypes.

3.3. Thermal Stability. To compare the thermal behavior of the three silver delafossite polytypes, we performed TGA analysis under the same conditions. As shown in Figure 6, up to 700 °C, the global trend is the same for the three polytypes, and two steps can be observed with an additional one at higher temperature as shown for the D2 polytype. In all cases there is first a very weak weight loss (<0.5%) from roughly 200 to 400 °C followed by a second and abrupt loss. In a recent study Muguerra et al.[25] explained the first weak loss by an oxygen departure from an initial overstoichiometric $AgCoO_{2+\delta}$ material. Without any supplementary data to confirm this hypothesis, we rather propose to

dx.doi.org/10.1021/ic2002354 |Inorg. Chem. 2011, 50, 4529–4536

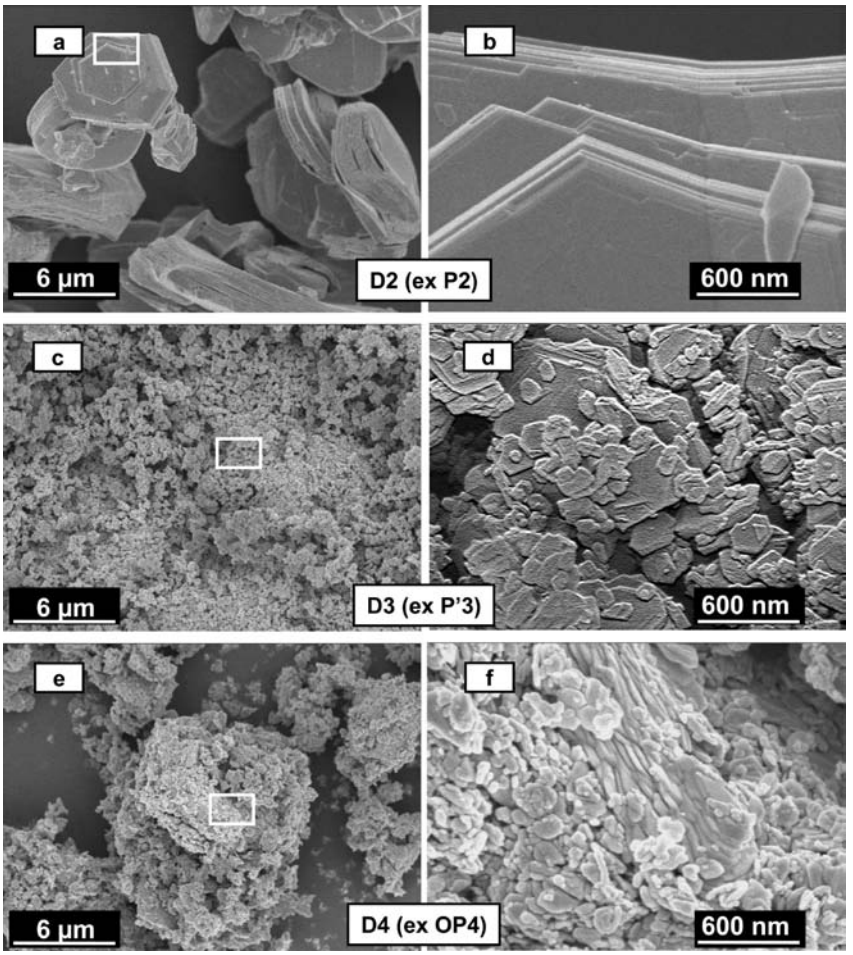

Figure 5. SEM micrographs of the $AgCoO_2$ polytypes D2 (a-b), D3 (c-d), and D4 (e-f) all obtained by ionic exchanges from respectively P2-$Na_{\sim 0.7}CoO_2$, P′3-$Na_{\sim 0.6}CoO_2$, and OP4-(Li/Na)CoO_2 (after ball-milling) precursors.

assign it to the evaporation of some water remaining from the washing step. The second weight loss is associated to the decomposition of the silver delafossites in metallic silver and Co_3O_4. In all cases, the mass losses are in reasonable agreement with the theoretical value of 5.4% corresponding to the oxygen departure related to the formation of silver metal and Co_3O_4. The presence of only these two decomposition products was further confirmed by XRD measurements (not presented here). As better seen from the inset in Figure 6, which shows the derivative curves of the TGA experiments, the decomposition begins at lower temperature for the D3 polytype and at higher temperature for the D2 polytype; the D4 case seems to be intermediate but closer to the one of the D3 polytype. Further heating only evidence the reduction of Co_3O_4 into CoO (see Figure 6 where a TGA measurement up to 800 °C is displayed for the D2 polytype).

The difference in the decomposition temperature could be related to the kinetic of the reaction in relation with the particle size of each sample. Such argument can explain the higher stability of the D2 polytype (bigger particles); however, it cannot explain the intermediate behavior of the D4 polytype which is characterized by the smallest particles and some intrinsic properties related to the weak structural differences between those three polytypes might also influence the thermal stability.

The kinetics of the decomposition is also related to the particle size distribution, and the trends observed with the TGA measurements are in agreement with the SEM results (Figure 5). Indeed, the narrow distribution of the particle size for the D2 polytype is reflected in the sharp peak of the derivative curves (inset of Figure 6) while the broad particle size distribution associated to the D3 and D4 polytypes is reflected in the broad temperature range for the decomposition (large peaks on the derivative curves, see inset of Figure 6).

3.4. Electrical Properties. Figure 7a shows that the temperature dependencies of the electrical resistivity are very similar for the three $AgCoO_2$ delafossites. The three polytypes display an insulator behavior with large resistivity values at room temperature (∼200, ∼720, and ∼980 Ω cm for D2, D3, and D4 polytypes, respectively).

The Seebeck coefficient is positive, and its temperature dependence follows a monotonic and roughly linear increase up to room temperature for the three polytypes (Figure 8).

Such behavior shows that charge carriers are holes diffusing through a hopping mechanism.

In the discussion of the present results we must keep in mind that the measurements were performed on non-sintered compacted pellets, the bulk density of which is about 70%. Another issue when measuring polycrystalline pellets is the 2D character of the structure that lets one expect a more or less important

dx.doi.org/10.1021/ic2002354 |*Inorg. Chem.* 2011, 50, 4529–4536

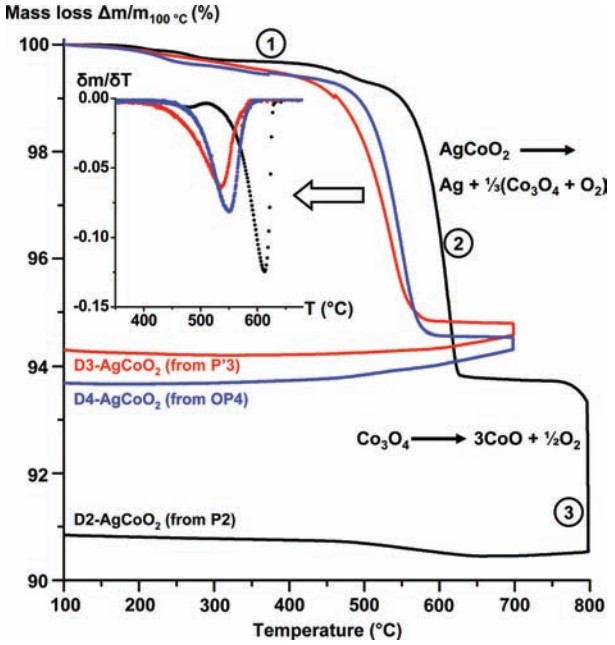

Figure 6. Thermogravimetric data for delafossite polytypes: D2-$AgCoO_2$ obtained from P2-$Na_{\sim 0.7}CoO_2$ (black line), D3-$AgCoO_2$ obtained from P′3-$Na_{\sim 0.6}CoO_2$ (red line), and D4-$AgCoO_2$ obtained from OP4-(Li/Na)CoO_2 (blue line). The mass loss no. 2 corresponds to the delafossite decomposition into silver metal and Co_3O_4 while the mass loss no. 3 refers to the reduction of Co_3O_4 in CoO. The derivative curves in the 350−680 °C range are shown in the inset.

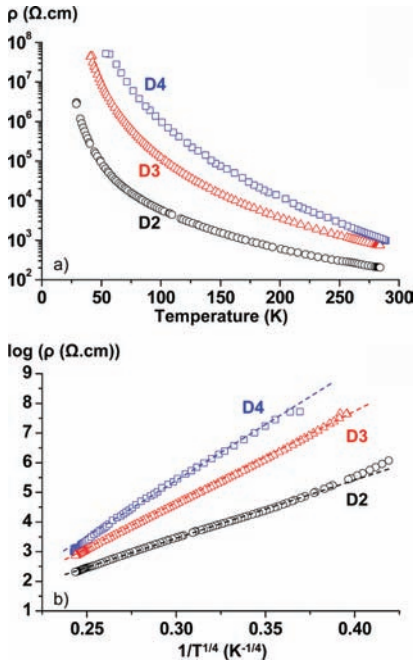

Figure 7. (a) Evolution vs temperature of the electrical resistivity measured on non-sintered compacted pellets of different $AgCoO_2$ delafossite polytypes: D2 (black circles), D3 (red triangles), and D4 (blue squares). In (b) The thermal activation can be also presented by a variable range hopping model plot $\log(\rho) = f(1/T^{1/4})$.

anisotropy of the electronic transport properties. Actually, this expectation is confirmed by measurements on some delafossite

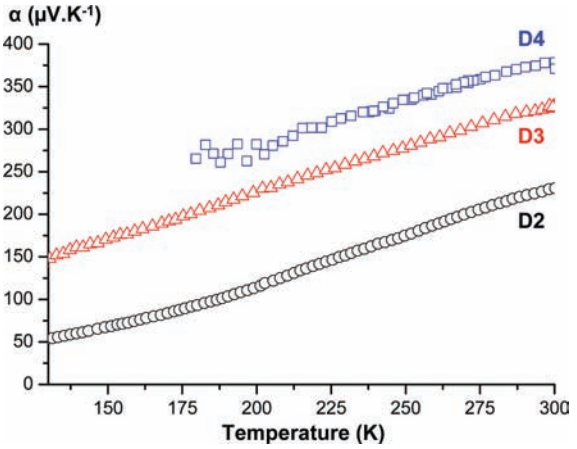

Figure 8. Evolution vs temperature from ∼130 to 300 K of the thermopower measured on non-sintered compacted pellets of different $AgCoO_2$ delafossite polytypes: D2 (black circles), D3 (red triangles), and D4 (blue squares). The too high resistivity below ∼130 K prevents measurement.

single crystals showing that the electrical resistivity along the crystallographic *c*-axis is larger than perpendicularly to it by 2 to 3 orders of magnitude[3] (For plate-like crystals, the electrical resistivity of polycrystalline pellets is dominated by the in-plane component). The average resistivity of our samples is much lower than the in-plane component of the electrical resistivity of D3 single crystals.[3] As recalled above, AMO_2 delafossites where A is a d^{10} element are insulators, whereas for d^9 A elements they are metallic. This result is simply explained by a crude band diagram where the conduction band arises from the overlap of hybridized d_{z^2}-s orbitals that spread out in the A-plane. This band is fully occupied for a d^{10} configuration whereas it is half occupied for a d^9 configuration. It is very broad, at least in the case of 4d and 5d elements and A-A distances of the order of 3 Å (actually, $PdCrO_2$ is one of the most conductive oxide despite its 2D character[41,42]).

In our electrical measurements the intrinsic range is obviously not reached at room temperature, and carriers are of extrinsic origin. A recently reported theoretical study of the electronic structure of $PdCoO_2$ and $PtCoO_2$[43] strongly support the idea that, at least for weak doping rates, carriers are moving in silver layers. For large doping rates, the question whether carriers are partly located in both Ag and Co layers or not remains open.

As shown in Figure 7b, the resistivity data obey a Mott's law of the form $\rho = A \exp[(T_0/T)^n]$. The exponent n was adjusted to $^1/_4$ to fit our data; such behavior is typical of 3D variable range hopping.[44,45] Such a mechanism is expected to become predominant at low temperature when the carriers are occupying states localized in the Anderson sense. T_0 $(\propto W \cdot (R/\zeta)^3)$[43] is increasing from D2 to D4 suggesting a decreasing localization length (ζ) or an increasing hopping distance (R) and/or an increasing hoping energy (W).

The magnitude of the thermoelectric power is, as expected from the resistivity trends at room temperature, higher for the most resistive D4-sample (∼380 μV K^{-1}) and lower for the less resistive D2-sample (∼240 μV K^{-1}). As compared to the $LiCoO_2$ layered polytypes that exhibit different electrochemical behaviors ascribed to different surroundings of CoO_6 octahedra,[39,44] the impact of the oxygen stacking on the properties of the three delafossites is dominated by the differences in doping rates. These differences could result from the differences

dx.doi.org/10.1021/ic2002354 |*Inorg. Chem.* 2011, 50, 4529–4536

in both the mechanical and the thermal treatments used for the synthesis of the precursors that could deeply impact on the products resulting from the ionic exchange. If we assume that the excess holes are localized on the cobalt atoms, the Heikes formula applied for the room temperature value (for low spin e^4a^2 and e^4a^1 electronic configurations for Co^{3+} and Co^{4+}, respectively[46]) gives around 2, 4, and 11% of carriers for the D4, D3, and D2 phases, respectively. If we suppose that our samples are pure single phases, that is, if we exclude the existence of amorphous or poorly crystallized impurity phase not seen through XRD, the ICP measurements discard an origin of the defects in silver vacancies as the Ag/Co ratio is close to unity. On the other hand, the TGA does not account for an oxygen excess in $AgCoO_{2+\delta}$ (as proposed by Muguerra et al.[25]) increasing from the D4 to the D3 and to the D2 phases.

Anyway, the measured electrical properties do not reflect the intrinsic peculiarities of the studied compounds, and it is necessary to improve the shaping of the materials to possibly draw conclusions about the influence of the oxygen stacking upon the physical properties of these delafossites. This work is now in progress.

4. CONCLUSION

A new polytype of $AgCoO_2$ delafossite was obtained by an ion-exchange process from the mixed ordered OP4-$(Li/Na)CoO_2$ precursor. This compound is the second example of new packing after O4-$LiCoO_2$[39,47] and demonstrates the interest of ionic exchanges from the ordered OP4-$(Li/Na)CoO_2$ to prepare new ordering of alternate layered $(A/A')CoO_2$ compounds.

As it was anticipated from a preliminary approach based on the ion-exchange mechanisms used for the synthesis of D2 and D3 polytypes, the structure of this new $AgCoO_2$ delafossite exhibits an ordering with alternating D2 and D3 blocks; 4 CoO_2 slabs are necessary for a complete description of the structure which corresponds to a D4-$AgCoO_2$ polytype. It crystallizes in the $P6_3/mmc$ space group with $a_{hex.} = 2.871(1)$ Å and $c_{hex.} = 24.448(1)$ Å.

The three polytypes exhibit a global insulating behavior and decompose in the same range of temperature. No clear conclusion could be drawn concerning the impact of the structure peculiarities on the physical properties.

AUTHOR INFORMATION

Corresponding Author

*E-mail: pollet@icmcb-bordeaux.cnrs.fr.

ACKNOWLEDGMENT

The authors want to thank J. Villot and S. Fourcade of technical assistance; P. Dagault for TGA analysis; L. Etienne for ICP-AES analysis and sample grain size measurements; E. Lebraud and S. Pechev for XRD acquisitions; C. Denage for SEM analysis; Agence National de la Recherche (OCTE project) and Région Aquitaine for financial support. CEA is also thanked for a scholarship for R.B.

REFERENCES

(1) Soller, W.; Thompson, A. *Phys. Rev.* **1935**, *47*, 644.
(2) Pabst, A. *Am. Mineral.* **1946**, *31*, 539.
(3) Shannon, R. D.; Rogers, D. B.; Prewitt, C. T. *Inorg. Chem.* **1971**, *10* (4), 713.
(4) Rogers, D.; Shannon, R.; Prewitt, C.; Gillson, J. *Inorg. Chem.* **1971**, *10* (4), 723.
(5) Prewitt, C.; Shannon, R.; Rogers, D. *Inorg. Chem.* **1971**, *10* (4), 719.
(6) Zheng, S.; Jiang, G.; Su, J.; Zhu, C. *Mater. Lett.* **2006**, *60* (29−30), 3871.
(7) Seshadri, R.; Felser, C.; Thieme, K.; Tremel, W. *Chem. Mater.* **1998**, *10* (8), 2189.
(8) Marquardt, M. A.; Ashmore, N. A.; Cann, D. P. *Thin Solid Films* **2006**, *496* (1), 146.
(9) Tanaka, M.; Hasegawa, M.; Takei, H. *J. Phys. Soc. Jpn.* **1996**, *65* (12), 3973.
(10) Hasegawa, M.; Higuchi, T.; Tanaka, M.; Tsukamoto, T.; Shin, S.; Takei, H. *Mater. Trans.* **2001**, *42* (6), 961.
(11) Wichainchai, A.; Dordor, P.; Doumerc, J.; Marquestaut, E.; Pouchard, M.; Hagenmuller, P.; Ammar, A. *J. Solid State Chem.* **1988**, *74* (1), 126.
(12) Shin, Y.; Doumerc, J.-P.; Dordor, P.; Pouchard, M.; Hagenmuller, P. *J. Solid State Chem.* **1993**, *107* (1), 194.
(13) Shin, Y.; Doumerc, J.-P.; Pouchard, M.; Hagenmuller, P. *Mater. Res. Bull.* **1993**, *28* (2), 159.
(14) Shin, Y.-J.; Kwak, J.-H.; Yoon, S. *Bull. Korean Chem. Soc.* **1997**, *18* (7), 775.
(15) Sörgel, T.; Jansen, M. *Z. Anorg. Allg. Chem.* **2005**, *631* (15), 2970.
(16) Schreyer, M.; Jansen, M. *Angew. Chem., Int. Ed.* **2002**, *41* (4), 643.
(17) Yoshida, H.; Muraoka, Y.; Sörgel, T.; Jansen, M.; Hiroi, Z. *Phys. Rev. B* **2006**, *73* (2), 020408.
(18) Hahn, H.; Lorent, C. D. *Z. Anorg. Allg. Chem.* **1957**, *290* (1−2), 68.
(19) Feitknecht, W.; Moser, K. *Z. Anorg. Allg. Chem.* **1960**, *304* (3−4), 181.
(20) Von Stählin, W.; Oswald, H.-R. *Z. Anorg. Allg. Chem.* **1969**, *367*, 206.
(21) Von Stählin, W.; Oswald, H.-R. *Z. Anorg. Allg. Chem.* **1970**, *373*, 69.
(22) Ishiguro, T.; Ishizawa, N.; Mizutani, N.; Kato, M. *J. Solid State Chem.* **1983**, *49* (2), 232.
(23) Delmas, C.; Fouassier, C.; Hagenmuller, P. *Phys. B+C (Amsterdam, Neth.)* **1980**, *99* (1−4), 81.
(24) Sheets, W.; Stampler, E.; Bertoni, M.; Sasaki, M.; Marks, T.; Mason, T.; Poeppelmeier, K. *Inorg. Chem.* **2008**, *47* (7), 2696.
(25) Muguerra, H.; Colin, C.; Anne, M.; Julien, M.-H.; Strobel, P. *J. Solid State Chem.* **2008**, *181* (11), 2883.
(26) Berthelot, R.; Pollet, M.; Carlier, D.; Delmas, C. *Inorg. Chem.* **2011**, *50* (6), 2420.
(27) Balsys, R.; Lindsay Davis, R. *Solid State Ionics* **1994**, *69* (1), 69.
(28) Ren, Z.; Shen, J.; Jiang, S.; Chen, X.; Feng, C.; Xu, Z.; Cao, G. *J. Phys.: Condens. Matter* **2006**, *18* (29), L379.
(29) Chen, X.; Xu, X.-F.; Hu, R.-X.; Ren, Z.; Xu, Z.-A.; Cao, G.-H. *Acta Phys. Sin.* **2007**, *56*, 1627.
(30) Bos, J.; Hertz, J.; Morosan, E.; Cava, R. *J. Solid State Chem.* **2007**, *180* (11), 3211.
(31) Fouassier, C.; Matejka, G.; Reau, J.-M.; Hagenmuller, P. *J. Solid State Chem.* **1973**, *6* (4), 532.
(32) Ono, Y.; Ishikawa, R.; Miyazaki, Y.; Ishii, Y.; Morii, Y.; Kajitani, T. *J. Solid State Chem.* **2002**, *166* (1), 177.
(33) Blangero, M.; Carlier, D.; Pollet, M.; Darriet, J.; Delmas, C.; Doumerc, J.-P. *Phys. Rev. B: Condens. Matter Mater. Phys.* **2008**, *77* (18), 184116.
(34) Doumerc, J.-P.; Ammar, A.; Wichainchai, A.; Pouchard, M.; Hagenmuller, P. *J. Phys. Chem. Solids* **1987**, *48* (1), 37.
(35) Ammar, A. . Ph.D. Thesis, University of Marrakech, Marrakech, Morocco, 1988
(36) Shivakumara, C.; Hegde, M. *Proc. Indian Acad. Sci. Chem. Sci.* **2003**, *115* (5−6 SPEC. ISS.), 447.
(37) Ussow, A. *Z. Anorg. Allg. Chem.* **1904**, *38* (1), 419.

(38) Dordor, P.; Marquestaut, E.; Villeneuve, G. *Rev. Phys. Appl.* **1980**, *15*, 1607.
(39) Berthelot, R.; Carlier, D.; Pollet, M.; Doumerc, J.-P.; Delmas, C. *Electrochem. Solid-State Lett.* **2009**, *12* (11), A207.
(40) Carlier, D.; Saadoune, I.; Croguennec, L.; Ménétrier, M.; Suard, E.; Delmas, C. *Solid State Ionics* **2001**, *144* (3−4), 263.
(41) Takatsu, H.; Maeno, Y. *J. Cryst. Growth* **2010**, *312* (23), 3461.
(42) Takatsu, H.; Yonezawa, S.; Fujimoto, S.; Maeno, Y. *Phys. Rev. Lett.* **2010**, *105* (13), 137201.
(43) Eyert, V.; Frésard, R.; Maignan, A. *Chem. Mater.* **2008**, *20* (6), 2370.
(44) Mott, N. F.; Davis, E. A.. *Electronic process in non-crystalline materials*; Clarendon Press: Oxford, 1979.
(45) Cox, P. *Transition metal oxides: an introduction to their electronic structure and properties*; Clarendon Press: Oxford, 1995.
(46) Pollet, M.; Doumerc, J.-P.; Guilmeau, E.; Grebille, D.; Fagnard, J.-F.; Cloots, R. *J. Appl. Phys.* **2007**, *101* (8), 083708.
(47) Komaba, S.; Yabuuchi, N.; Kawamoto, Y. *Chem. Lett.* **2009**, *38* (10), 954.